

## Profiles of Electron Density in the Lower Ionosphere Observed by the MU Radar

Xun-Jie ZHANG<sup>1</sup>, Xue-Qin RUAN<sup>1</sup>, Toru SATO<sup>2</sup>,  
Iwane KIMURA<sup>2</sup>, Shoichiro FUKAO<sup>3</sup>, and Susumu KATO<sup>3</sup>

<sup>1</sup> *Wuhan Institute of Physics, Academia Sinica, Wuhan, Hubei, China*

<sup>2</sup> *Department of Electrical Engineering II, Kyoto University, Kyoto 606, Japan*

<sup>3</sup> *Radio Atmospheric Science Center, Kyoto University, Uji, Kyoto 611, Japan*

(Received March 2, 1990; Revised November 8, 1990)

The middle and upper atmosphere radar of Japan is a 46.5 MHz, monostatic pulse-Doppler radar with an active phased-array antenna which consists of 475 crossed Yagis. Since 1983, observations of irregularities in the troposphere, stratosphere, mesosphere, and ionospheric *F*-region have been conducted. Here we will show that the MU radar can be used to get the electron densities of the ionospheric *E*-region of 90 to 160 km height as well. Preliminary results are presented. We compared variations of electron density at different heights for a normal day on September 22, 1987 and for a partial eclipse on September 23, 1987. For the partial eclipse day, the electron densities in the whole *E*-region began to decrease at around 1030 JST. The duration was about 3 hours, and the decrease of electron density was about 20% relative to a normal day. These results showed that electron densities directly reflect the variation of the solar UV flux.

### 1. Introduction

The Japanese middle and upper atmosphere (MU) radar is located at Shigaraki (34.85°N, 136.10°E). This system has been described in detail by FUKAO *et al.* (1985a, b), as the techniques and capability of ionospheric incoherent scatter measurements were by SATO *et al.* (1989). Many important results have been obtained from the respective measurements. OLIVER *et al.* (1988a, b) studied the *F*-region electrodynamics and the effects of a large magnetic storm on February 6–8, 1986 by MU radar data. SARYO *et al.* (1989) explained a midday bite-out event of the *F* layer.

LALONDE (1966) analyzed profiles of electron density from 50 to 400 km using the Arecibo 430 MHz radar, Puerto Rico. He pointed out that the absolute electron density could be 20% lower if the correction was performed by normalizing the backscatter power profile to the *E*-region critical frequency. RASTOGI and BOWHILL (1975) also gave profiles of electron density in the lower ionosphere using the incoherent scatter radar. These results were consistent with the results by rocket measurements.

For the measurement of faint incoherent scatter signals, the existence of stronger background noise and coherent scatterings for the MU radar operating frequency has an equivalent effect as reducing the S/N ratio. It is very disadvantageous for the incoherent scatter measurements, specially for power measurements in the lower ionosphere, for which frequent contaminations due to meteor and sporadic *E* echoes are serious. This had been the major reason which prevented a successful measurement of the lower

Table 1. Basic parameters of the MU radar

parameter	values
Operational frequency	46.5 MHz
Antenna	active phased array, 103 m diameter circular array of 475 crossed Yagis
aperture	8330 m <sup>2</sup>
steerability	steering is possible in each IPP
Transmitter	475 solid state amplifiers
peak power	1 MW
average power	50 KW
pulse length	1–512 $\mu$ s
IPP	400–65000 $\mu$ s
pulse compression	up to 32 bit binary phase coding Barker and complementary codes in use
Receiver	
bandwidth	1.65 MHz
dynamic range	70 dB
IF	5.0 MHz

ionosphere by the MU radar.

However, we found that as we operate the MU radar continuously, it is always possible to find some data in which the contaminations are weak enough to derive the electron density. Although it requires experience and morphological knowledge in ionospheric observations, we may be able to discriminate these profiles by eye to select good ones for the electron density determinations.

The aim of this paper is to answer whether the profiles of electron density in the lower ionosphere can be derived from the MU radar data.

## 2. Data Processing

Table 1 shows the basic parameters of the MU radar. In order to make the most efficient use of the MU radar function, several observation modes for the incoherent scatter measurement were used (SATO *et al.*, 1989). Here we used data observed by the power mode. This mode usually adopts a 7 bit Barker-coded pulse with 64-microsecond subpulses, which provide a range resolution of 9.6 km. The direction of the antenna beam was tilted by 20° from the zenith, with the azimuthal angles of 85°, 175°, 265°, and 355°, corresponding to the geomagnetic east, south, west, and north directions, respectively. It should be pointed out that the MU radar can alter the antenna beam directions every IPP, providing important information about the spatial variations of electron density. So it is very advantageous to observe electron densities at different directions simultaneously.

We analyzed the four data sets: September 21–24, 1987, July 7–11, 1988, January 7–10, 1989, and March 6–9, 1989. For the above data, we first derived the electron density profiles from 77 to 1157 km following the data processing procedure developed by SATO *et al.* (1989). The power profile was normalized by the ionospheric  $F$  critical frequency. The average profiles for 15 and 60 min were usually taken. We compared

the different profiles in regular sequence under the quiet ionospheric conditions to investigate whether the receiver gain changes during the observed period. The results showed that these profiles were very consistent with each other. It could mean that the interferences were sufficiently weak and the receiver gain was stable. We consider that these data are good enough for our purpose of deriving the electron density.

For the MU radar operating frequency, the wave length  $\lambda$  is much greater than the Debye radius  $D$  in the plasma. Therefore, interactions of the Coulomb force between electrons and ions can influence the fluctuations of the electron density. The scattering cross section depends on the ratio of the electron and the ion temperatures  $T_r$ . When  $\lambda^2 \gg 4\pi^2 D^2$ , the collective plasma scattering cross section can be expressed as (BUNEMAN, 1962)

$$\sigma = N_e \sigma_o \frac{1}{1 + T_r}, \quad (1)$$

$$\sigma_o = \frac{8\pi}{3} r_o^2 \quad (2)$$

where  $N_e$  is the electron density, and  $r_o$  is the classical radius of an electron. The scattered power is given by (SATO *et al.*, 1989)

$$P_s = \frac{C}{1 + T_r} N_e \quad (3)$$

where  $C$  is a constant associated with the system parameters of the MU radar. We can see from Eq. (3) that  $P_s$  decreases by 33% if  $T_r$  increases from 1 to 2.

The value  $T_r$  is smaller in the lower ionosphere than in the upper ionosphere. The diurnal variation of  $T_r$  at the  $F$  peak height at Shigaraki has been measured by SATO *et al.* (1989). Its value equates 1 at night time, but it rapidly increases to 2 after sunrise. The  $T_r$  value depends also on the solar and geomagnetic activities. LALONDE (1966) considered that  $T_r$  of the lower ionosphere was of the order of 1.5 during daytime, and drops to 1 at nighttime. However, in the lower ionosphere, the relaxation time of the temperature is very short due to high collision frequencies, typical values being  $10^{-4}$  and 1 sec at 90 and 150 km, respectively. So the  $T_r$  value is close to 1 in the  $E$  region height.

We compared two methods of deriving electron density profiles using different normalizations. One is by the peak electron density in the  $F$  region, and the other by that in the  $E$  region. When we adopted the normalization by the latter, the value of the electron density at the  $F$  peak height became lower than the corresponding value determined by the  $F$  critical frequency of the ionogram at Shigaraki. Usually, the deviations were 40-50%. We could thus estimate  $T_r$  at the  $F$  region peak height to be ranging from 2.3 to 3.3.  $T_r$  was within 2.0 to 2.5 during the daytime, but raised to 3.3 after sunrise. The high value after sunrise seems to be explained by the fact that the peak height of the  $F$  region goes up to a higher altitude after sunrise, where the electrons are heated by photoelectrons, whereas the ion temperature is less sensitive to heating due to the photoelectrons (*e.g.*, BANKS and KOCKARTS, 1973). Based on the ionogram taken at Kokubunji, Japan ( $35^\circ 42'N$ ,  $139^\circ 29'E$ ), the peak height of the  $F$  region indeed showed an elevation of a few tens km just after sunrise. It then decreased to a stable daytime level, and further decreased toward sunset.

January 7–8, 1989

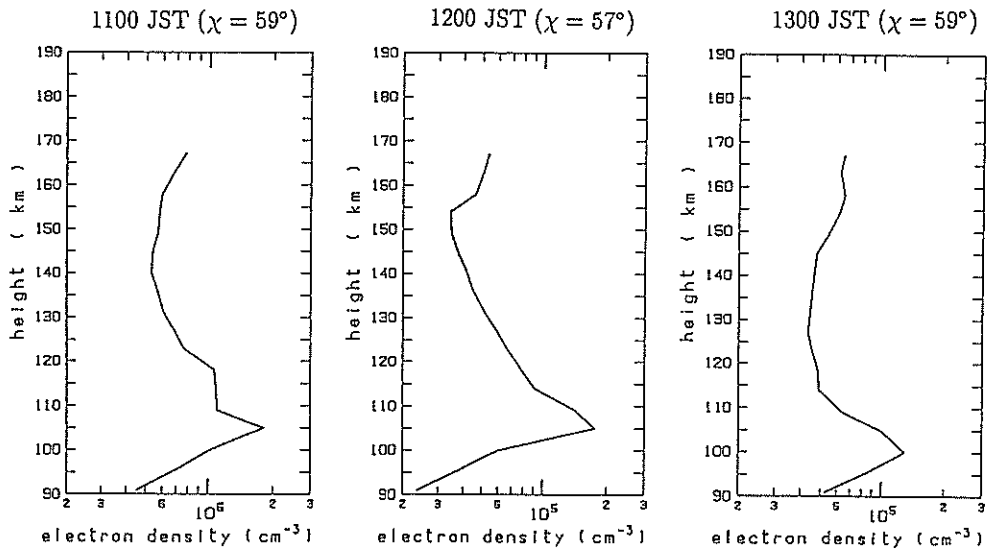


Fig. 1. The average profiles of electron density in January 9–10, 1989 for three local times.

These results showed that the profiles of electron density derived by the MU radar are reasonable. The deviations of the electron density were caused by the variations of temperature with height. All profiles used in this paper were normalized by the peak electron density in the *E* region.

We also tried to analyze some data during the nighttime. The derived electron densities, however, were one order of magnitude higher than the results of the rocket, and were not reliable as discussed in the next section.

### 3. Results and Discussion

Figure 1 shows several examples of the electron density profiles averaged for two days from January 7–8, 1989. We can see from this figure that there is an obvious peak in the *E* region, with an electron density of about  $2 \times 10^5 \text{ cm}^{-3}$  around 1200 JST. The wide valley between the *E* and *F* regions can be denoted. The electron density varied monotonically in both, above and below the peak. The altitude of the maximum electron density gradually decreased from 104 km in the morning to 99 km in the afternoon. These height variations of the peak showed good agreement with those seen in ionograms during the winter.

Figure 2 shows similar profiles from September 21–24, 1987. The shape of these profiles showed very smooth variations with height above the peak, and the valley was not clear, showing different characteristics to Fig. 1. We found that the cylinder electron contents from 90 to 160 km was larger in September than in January, but the peak value of the electron density in the *E* region was higher in January than in September.

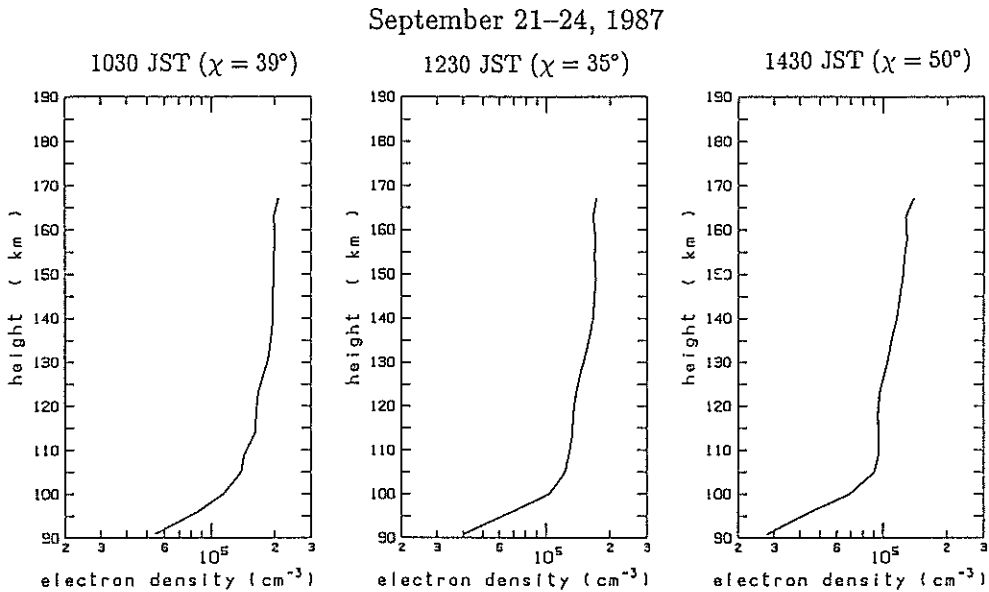


Fig. 2. The average profiles of electron density on September 21–24, 1987.

We also analyzed profiles during March 6–9, 1988 and July 9–12, 1988. In general, the profiles of March, 1988 were similar to Fig. 1, whereas the profiles of July, 1988 were to Fig. 2. They could represent two kinds of typical profiles observed over Shigaraki, Japan.

In order to examine such difference between these two types of profiles, we compared our results with a model of the *E-F* valley derived from ionosonde observations. Since the valley produces a non-trace region in the ionogram, one needs to investigate a method to extract the valley ionization from the virtual height. HUANG and TAN (1985) proposed an improved method to estimate profiles of the valley based on the technique developed by LOBB and TITHERIDGE (1977). They assumed that the electron density profile in the valley is represented by a superposition of a positive and a negative parabolic profile, which imposes less limitation to the shape of a profile than the method of Lobb and Titheridge.

Figure 3 gives the variations of model parameters of the valley obtained by this method with the solar zenith angle  $\chi$ . The width of the valley,  $W_v$ , specifies the distance from the *E*-region peak to the *F*-region base, and the depth  $R$  is represented by

$$R = \sqrt{1 - \left(\frac{f_b}{f_{oE}}\right)^2},$$

where  $f_b$  is the frequency of the valley bottom, and  $f_{oE}$  is the critical frequency of the *E*-region. This figure shows that when  $\chi$  varies from  $70^\circ$  to  $40^\circ$ , the depth of the valley lies in a range of 0.2–0.25, which corresponds to a shallow valley. The valley vanishes for  $\chi < 30^\circ$ . In contrast, a deep valley appears during sunrise and sunset hours. Recent

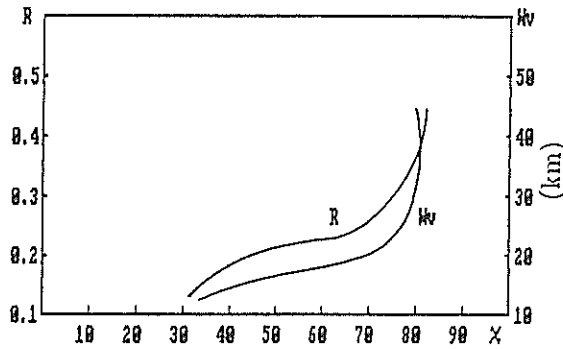


Fig. 3. Variations of the depth  $R$  and the width  $W_v$  of the  $E$ - $F$  valley versus solar zenith angle  $\chi$  as predicted by a model.

results by HUANG *et al.* (1987) confirmed this model. We can also see that the width of the valley also changed largely with the solar zenith.

The observed profiles by the MU radar shown in Figs. 1 and 2 seems to indicate a much larger sensitivity of the valley depth on the solar zenith angle than predicted by the model, although their tendency was consistent with what was expected from the difference of the solar zenith angle. The valley was almost non-existent for the September data when  $\chi$  is  $35$ – $50^\circ$ , while  $R$  was larger than  $0.5$  for January data with  $\chi$  of  $57$ – $59^\circ$ . Part of this discrepancy is attributed to the fitting method used by the model calculation. Since the method always assumed the existence of the valley in the fitting procedure, it tended to over-estimate  $R$  for small  $\chi$  values. As for the profiles obtained by the MU radar, there is some possibility that the  $E$ -region peak electron density was over estimated due to contaminations by weak meteor echoes. Further compilation of data is necessary to examine the dependence of the valley structure on other parameters such as the solar activity.

Next we derived a set of profiles on September 22, 1987 for different heights to study the variations of electron density with the solar zenith. These results are shown in Fig. 4(a). The peak electron density in the  $E$  region is also given in this figure. We also noted from these diurnal variations that the maximum values of the electron density for different heights appeared at different times. The electron density of the  $140$ – $153$  km region increased faster and showed its maximum earlier than other heights. We calculated the variations of the electron density maximum with the solar zenith, which is in agreement with Chapman's formula.

Figure 4(b) is the results of a partial eclipse on September 23, 1987. The eclipse started at Shigaraki at 1000 JST, and ended at 1255 JST. The maximum coverage during the eclipse was of about 60%. As can be seen from this figure, the electron densities at different heights decreased simultaneously after about 1030 JST. The influence of the partial eclipse lasted for 3 hours. The electron density decreased 20% relative to that of a normal day. The time variation of these profiles showed a good agreement with that of the solar UV flux, which suggests that the electron density of the lower ionosphere is controlled directly by the solar radiation.

Finally we examined the accuracy in the determination of the electron density. In

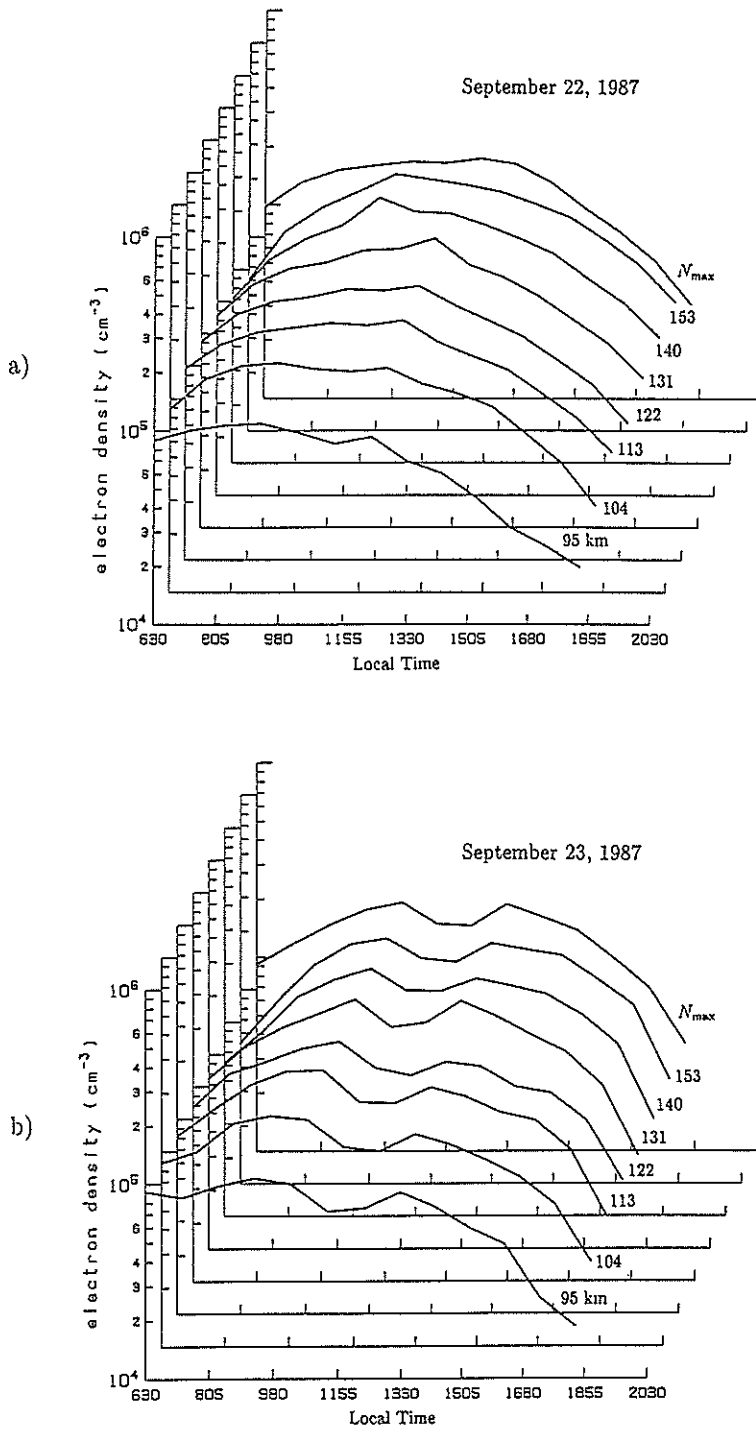


Fig. 4. Variations of the electron density with time and height. (a) on a normal day of September 22, 1987, (b) on a partial eclipse day of September 23, 1987.

the beginning of this research, we analyzed a large number of records including ranges from 80 to 90 km. However, the derived electron densities below 90 km were one order of magnitude higher than those obtained by rockets. The deviation was larger in the morning than in the afternoon, which indicates that contaminations are dominated by weak meteor echoes. The data from the night time were also analyzed. The deviations were even larger. Although some efforts to decline the low limitation value were made by improving noise reduction schemes, the improvements were not distinct.

The lower limit of the electron density measurement imposed by these interferences is on the order of  $10^4 \text{ cm}^{-3}$ . We therefore compared only daytime results above 90 km, which agreed with the rocket measurements.

Among other sources of error,  $T_r$  is an important factor. EVANS (1965) compared different observations of temperature including radar, rocket, and satellite information. The conclusion was that below about 130 km the  $E$  region is in a thermal equilibrium, but  $T_r$  could be in a range from 1.1 to 1.2 at 160 km. Since our analyses assumed that  $T_r = 1$  in the  $E$  region, the electron density normalized by the  $E$  region peak could cause an error of 10%.

We also examined errors in reading  $f_oE$  from ionograms. If the reading error is 0.1 MHz, then the electron densities in the lower ionosphere could produce a 7% error.

The lower ionospheric response to the solar flare is very prompt and conspicuous. If the absorption in the lower ionosphere is not negligible, it may affect the observed echo power profile. We computed the absorption for the quiet and disturbed conditions. Although the absorption can be 7 dB higher in the disturbed condition than in the quiet one, 92% of the absorption occurs below 80 km (ZHANG *et al.*, 1989). Since we normalized the power profiles to the maximum electron density in the  $E$  region, this effect could be neglected.

#### 4. Summary

In this report, we have presented the first result of the lower ionosphere observations made with the MU radar. The profiles of the electron density and their variations with time were derived. Major results are summarized in the following.

1) The profiles of the daytime electron densities from 90 to 160 km can be obtained using the MU radar data. The result obtained during a partial eclipse showed that these profiles directly reflect variations of electron density caused by the solar UV flux decrease.

2) The  $E$ - $F$  valley structure shows a large difference depending on the period of observation. The difference was larger than the expected by that of the solar zenith angle based on a model computation.

3) The lower limit of the observable electron density was limited by contaminations mainly due to weak meteor echoes. The magnitude of the contamination is on the order of  $10^4 \text{ cm}^{-3}$ . Attempts to obtain nighttime electron density in the  $E$  region were not successful.

The authors wish to thank the staff in charge of Prof. I. Kimura's laboratory, Department of Electrical Engineering II, Kyoto University for their helpful support. They are indebted to the staff of the Radio Atmospheric Science Center, and Data Processing Center, Kyoto University for their support in providing and in processing the data.



The MU radar belongs to, and is operated by the Radio Atmospheric Science Center, Kyoto University. Part of the data processing was performed at the Data Processing Center, Kyoto University.

## REFERENCES

- BANKS, P. M. and G. KOCKARTS, *Aeronomy*, Academic Press, New York, 1973.
- BUNEMAN, O., Scattering of radiation by the fluctuations in a nonequilibrium plasma, *J. Geophys. Res.*, **67**, 2050-2053, 1962.
- EVANS, J. V., Midlatitude ionospheric temperature on magnetically quiet and disturbed days, *J. Geophys. Res.*, **70**, 2726-2732, 1965.
- FUKAO, S., T. SATO, T. TSUDA, S. KATO, K. WAKASUGI, and T. MAKIHIRA, The MU radar with an active phased array system. 1. Antenna and power amplifiers, *Radio Sci.*, **20**, 1155-1168, 1985a.
- FUKAO, S., T. TSUDA, T. SATO, S. KATO, K. WAKASUGI, and T. MAKIHIRA, The MU radar with an active phased array system, 2. In-house equipment, *Radio Sci.*, **20**, 1169-1176, 1985b.
- HUANG, X. Y. and Z. X. TAN, Profiles of ionograms containing a valley, *ACTA Geophys. Sinica*, **27**, 504-510, 1985.
- HUANG, X. Y., Y. Z. SU, and Z. X. TAN, A method to extract information in non-trace region of ionogram, *ACTA Geophys. Sinica*, **30**, 341-348, 1987.
- LALONDE, L. M., Incoherent backscatter observations of sporadic E, *J. Geophys. Res.*, **71**, 5059-5065, 1966.
- LOBB, R. J. and J. E. TITHERIDGE, The valley problem in bottomside ionogram analysis, *J. Atmos. Terr. Phys.*, **39**, 35-42, 1977.
- OLIVER, W. L., S. FUKAO, T. SATO, T. TSUDA, S. KATO, I. KIMURA, A. ITO, T. SARYO, and T. ARAKI, Ionospheric incoherent scatter measurements with the MU radar: Observations during the large geomagnetic storm of 6-8 February 1986, *J. Geophys. Res.*, **93**, 14649-14655, 1988a.
- OLIVER, W. L., S. FUKAO, T. SATO, T. TSUDA, S. KATO, I. KIMURA, A. ITO, T. SARYO, and T. ARAKI, Ionospheric incoherent scatter measurements with the MU radar: Observations of F-region electrodynamics, *J. Geomag. Geoelectr.*, **40**, 963-985, 1988b.
- RASTOGI, P. K. and S. A. BOWHILL, Remote sensing of the mesosphere using the Jicamarca incoherent-scatter radar, *Aeron. Rep.*, **68**, 241pp, 1975.
- SARYO, T., M. TAKEDA, T. ARAKI, T. SATO, T. TSUDA, S. FUKAO, and S. KATO, A midday bite-out event of the F2 layer observed by MU radar, *J. Geomag. Geoelectr.*, **41**, 727-734, 1989.
- SATO, T., A. ITO, W. L. OLIVER, S. FUKAO, T. TSUDA, S. KATO, and I. KIMURA, Ionospheric incoherent scatter measurements with the MU radar: Techniques and capability, *Radio Sci.*, **24**, 85-98, 1989.
- ZHANG, X. J., X. Q. RUAN, H. A. LIN, and L. ZHANG, Several effects of the lower ionosphere by solar flare, *Chinese Solar-Geophys. Data*, Special Issue **2**, 117, 1989.